REPORT

Contact person
Gunnar Kjell
SP Structural and Solid Mechanics
+46 10 516 52 23
gunnar.kjell@sp.se

Date: Jul. 2, 09
Reference: P903347 Rev.2a
Page: 1 (9)

Svensk Kärnbränslehantering AB
Kapsellaboratoriet
Box 925
572 29 OSKARSHAMN

Residual stress measuring by incremental hole drilling technique

(4 appendices)

This is a revised report. A new Appendix 4 has been included in the report. This appendix contains the measured stresses converted to the global coordinate system of the insert tube. The reason for doing this conversion was that the results from this measurement should be presented in the same manner as the results from a measurement done with the Deep-hole Drilling technique. The latter results are presented in Ref. [9]

A second revision of the report is done. In this revision calculated stresses in Appendix3 and 4 are considered to be unreliable if the corresponding von Mises effective stress is larger than 70% of the yield stress. All such calculated stress values are now shaded in both appendices. Some minor typing errors are also corrected. A wrong reference in this revision is corrected in Rev2a.

1 Test object

A half BWR insert tube Ø950 mm and 2000 mm long. The sample was marked I56.

The test sample was selected by the customer and sent to SP. It arrived to SP April 15, 2009.

2 Assignment

The objective was to carry out residual stress measurement at different locations on the envelope surface of the test sample.

3 Summary

From the measured strains residual stresses were calculated by the method outlined in the ASTM Standard procedure E837, Ref. [3]. It was then found that the requirements for a uniform residual stress field given in the standard were not fulfilled and therefore the stresses were calculated with the Integral Method described in Ref. [5]. This method is suggested in Ref [7] for highly non-uniform stress distributions. The calculations were done by a computer program written by G.S. Schajer, Ref. [6].

The reported stress values refer only to the test sample sent to SP.

4 Date of the measurement

The measurement was done during week 19 and 20, 2009.

5 Locations of the measuring points

A schematic sketch showing the insert tube and the measuring locations is given in *Figure 1*. The layout of the strain gages are shown on *Figure A3:1* in *Appendix 3*.

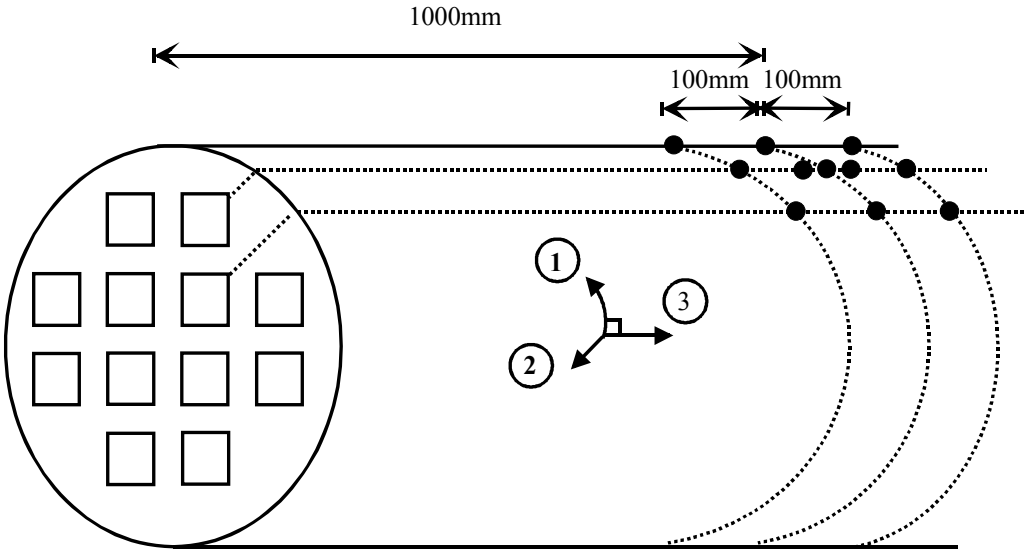

Figure 1 A schematic sketch of the insert tube showing the location of the measuring locations and the orientations of the three strain gages. The gages in the upper line are from left 1, 2 & 3, in the middle line 4, 5a, 5, 5b & 6 and in the lower line 7, 8 & 9.

During the drilling at location 5 the reading from the strain gages suddenly increased with a large step. This was probably caused by bending from the cutter when it hit some hard inclusion in the material. The measuring was aborted and a new measurement 15mm to the left was done. Even this measuring was disturbed and a third measuring was done 15mm to the right of the original point 5.

6 Equipment used at the measurement

A Milling Guide Model RS-200 from Measurements Group was used for drilling the holes. According to recommendation from the supplier of the equipment a high-speed air turbine and carbide-tipped 1.6mm cutters were used.

The strains were measured by CEA-06-062UL-120 gages. This type of gages is manufactured by the supplier of the hole drilling equipment and recommended for this type of tests.

The strains were sampled to a computer by an MGCPlus data acquisition system from HBM equipped with an AP814 and an ML801 card for conditioning and sampling single strain gages.

Photographs from the measurement and sketches of the hole drilling equipment are given in *Appendix 1*.

7 Implementation of the measurement

- The strain gages were bonded to the test sample according to instructions from the strain gage manufacturer. To minimize effects of temperature changes in the lead wires, three-wire quarter-bridge circuits were used.

- Before the drilling was started it was checked that all three gages gave stable reading on the data acquisition system.

- The stand for the drilling equipment was cemented to the sample and aligned with respect to the centring marks of the strain gage rosette.

- The drilling was done in 15 steps from zero hole depth down to 1.91 mm (slightly deeper than the hole diameter). For each increment the strains were sampled to the computer and stored in an EXCEL-sheet. When the strain was measured the drill was retracted from the hole.

- After the drilling was completed it was checked that the readings of the strain gages were stable.

- After the completion of the drilling the hole diameter was measured in three directions and a mean value of the measurements calculated and used in the analysis.

8 Material data

In the analysis material data according to *Table 1* were used. The data was given to SP by SKB and can be found in Ref:s [1] and [2].

Table 1: Material data used in the calculations.

Material	Young's modulus	Poisson's ratio	Yield stress
BWR (Nodular Cast Iron EN 1563; SKBdok 1064461)	166 GPa	0.30	274 MPa

9 Uncertainty in reported values

There are a lot of uncertainties in these types of investigations. Errors due to deviation in instrument reading and uncertainties in the used material data are in most cases small and their influence on the final result is also rather easy to estimate. When doing measurements with the hole drilling method it is essential that the drilling is very soft so no additional residual stresses are introduced and that no heating of the material occur. These types of errors are much more difficult to estimate as they are to a relative large amount depending on the skilfulness of the person doing the drilling. In this application the stress distribution was non-uniform and a calculation of the stress gradient had to be done by a commercial computer program. According to the manual for this program the calculations require engineering judgment. Below we have listed possible errors and discussed them briefly. The order of the different errors is the order of the different moments in the measurement.

Bonding and alignment of the strain gages

If the gages are not properly bonded to the target their deformation will not correspond to the deformation of the target and inaccurate readings are obtained. Poor bonding to the target can be present from the beginning of the measurement or the gages can loosen during the measurement. The person responsible for the bonding of the gages at this project is very experienced in this type of work. In other projects SP has bonded redundant gages to the test object and we have compared their readings and only found deviations of some microstrains, i.e. close to the resolution of the measurement system.

In this project it was rather easy to bond the gages as the samples were large and lying on a working desk. After terminating the measurement we checked the bonding of some of the gages by scraping them by a knife and got no indication of poor bonding.

Each gage element consists of three gages and the element should be aligned on the sample in order to be able to evaluate the strains in well defined directions. If the element is not properly aligned the calculated values of the direction of the principal stresses will be wrong, but their values will still be correct. The misalignment of a gage and then the fault in the direction of the calculated principal stresses should be within a few degrees.

Positioning and fixing the stand of the drilling equipment to specimens

The hole must be drilled in the centre of the gage element. On the foil with the gages the centre is marked by a circle with a diameter very close to the diameter of the cutter. By inserting a special-purpose microscope in the stand it was possible to, by X-Y-adjusting screws position the guide over the centre of the gage element. It was also easy to after the drilling check that the hole was drilled centrally. According to the manufacture of the drilling equipment, Ref. [4], the errors in calculated stresses due to inaccurate alignment should be less than 3 %.

The stand of the drilling equipment must be very rigidly fixed to the sample when the hole is drilled. The stand has three feet which are mounted in pads cemented to the sample. After doing a drilling and measurement these pads had to be removed and used at the next measurement location. This was done by striking them in a transverse direction. If the pads had been poorly cemented to the surface of the sample, it should be observed when they were removed. No such fault was observed.

Detection of the zero depth

The zero depth is the point at which drilling into the sample is started and the entire gage backing has been removed. This source of error is discussed in Ref. [7] but no estimate of the size of the error is given.

At this project the gage backing material was carefully removed by a hand operated drill and when this was done the special-purpose microscope was positioned in the stand and it was checked that the zero depth was achieved.

Even if the gage backing is correctly removed errors due to inaccurate alignment, concave profile of the drill cutting edge, axial clearance in the drill motor bearings and the surface roughness can cause errors in the determination of the zero depth.

These types of errors can lead to serious degradation in the quality of the first stress data.

By calculating the residual stresses with slightly different hole depths (simulating errors in detection of the zero depth) SP has found that the errors in the first stress data can be 5 %, but the error decreases rapidly with increasing hole depth.

Drilling the hole

This is another critical moment of the measurement. It's well known that heating of the material during the drilling and / or bending in the cutter can give inaccurate results. Before we started this project we discussed the implementation of the measurement with supplier of the milling equipment. Their recommendation was to use a high speed air turbine (400000 rpm), carbide tipped cutters (diameter 1.6mm), a slow feed rate of the cutter and to use a new cutter for each hole. We have followed these recommendations.

The drilling depth should be measured at each increment. This was done by a micrometer built into the drilling equipment. According to Ref. [8] this type of error is negligible in commercial systems. By simulating errors in the reading of the hole depth SP has also found that these errors are less than 1-2 % for all calculated stresses with exception for the stress just below the surface.

It is well known that hole drilling in cast iron is difficult. A hole will pass through different phases of the material and this can cause sudden changes in the measured strains. Some of the measurement series showed large jumps and these results are not presented in this report.

Measuring strains

Errors in measured strains can be due to errors in instrument reading or temperature drift in the strain gages or the lead wires to the gages. The bridge amplifier, used at the measurement, is annually calibrated and its inaccuracy is less than 1 %.

To reduce temperature drift we used three wire connection of the gages to the amplifier and used temperature compensated gages. Before and after the drilling of each hole we observed the reading from the gages during several minutes and made sure that they were stable. This indicates that the measured strains didn't change due to temperature fluctuations.

The errors in the reported stress values due to errors in the measured strains are therefore small; Ref. [8] estimates the error to be less than 5 %.

Measuring the hole dimensions

The hole dimension was measured by an optical head placed in the drilling rig and the hole diameter was measured in three direction and a mean-value of these measurements calculated. The reading was done against an optical scale. By measuring the hole diameter in three directions it was also checked that a circular hole was obtained. The deviation in diameters measured in three directions was less than less than 2 %. Ref. [8] states that this type of error is negligible

Material data used by the computer program

According to Ref. [8] the error due to uncertainties in the Young's modulus, E, is estimated to be less than 1 % and the error due to uncertainties in the Poisson's ratio, ν, to be less than 3 %.

Evaluating stresses from measured strains

As mentioned in the summary the stresses were calculated by the Integral Method as this method has the greatest capacity of resolving fine details. However, this method is sensitive to strain measurement errors.

A commercial computer program, written by a world leading expert in field Ref. [6], has been used. The software has a built in regularization for smoothing the calculated stresses and thereby reducing the effect of experimental errors when using the Integral Method.

A middle choice between using the Integral method and calculating uniform stresses is to use the Power method. This method involves averaging and is then less sensitive to experimental errors. But when this method was checked by looking at the misfit between the measured strains and the strains corresponding to the obtained stress solution was rather great. Therefore the method was not used.

According to the manual to the computer program Ref. [6], "*the nature of the residual stresses being measured is generally not known in advance, the choice of calculation method to be used is difficult to predict. A good strategy is to try all three methods in reverse order (Integral, Power Series, and Uniform Stress). Again, good engineering judgment, combined with a knowledge of the stresses expected, should be used to choose the most appropriate stress calculation method. Similar judgment is also essential when interpreting the meaning and reliability of the results obtained*"

It should also be mentioned that the accuracy of the calculated stresses decrease with the distance from the surface. The used computer program does not calculate stresses at greater deep than 1 mm.

Errors when the calculated residual stresses are not considerable lower than the yield strength

The calculation of stresses from measured strains requires that the material is linear elastic, i.e. yielding may not occur. If yielding occurs the calculated residual stresses will be too large. ASTM Standard procedure E837, Ref. [3], recommend that the calculated stresses should be less than 50 % of the yield stress whilst the manufacture of the drilling equipment, Ref. [4], suggest a limit of 70 %.

The yield stress has been determined to be 274 MPa for the sample. SP has used the von Mises effective stress as yielding criterion and assumed that calculated stresses are reliable if the corresponding von Mises stress is less than 70 % of the yield stress. If the von Mises stress is larger, the calculated stresses should be regarded to be uncertain. Such values are shaded in the tables with results in *Appendix 3* and *Appendix 4*

Table 2 A summary of the discussion about the uncertainties in the reported stress values

Type of error	Uncertainty	Remarks
Bonding and alignment of the strain gages	Strain values: Negligible Direction of principal stresses: < a few degree	Estimated by SP
Positioning and fixing the stand of the drilling equipment to specimens	<3 %	Ref. [4]
Detection of zero depth	<5 % (only important for stresses just below the surface)	Estimated by SP
Drilling the hole (measuring hole depth)	Negligible (or <2%)	Ref. [8] (Estimated by SP)
Measuring strains	<5 %	Ref. [8]
Measuring the hole dimensions	Negligible	Ref. [8]
Error in the Young's modulus, E	1 %	Ref. [8]
Error in the the Poisson's ratio, ν,	3 %	Ref. [8]
Evaluating stresses from measured strains	±15 % [1)]	Ref. [8]
Errors when the calculated residual stresses are not considerable lower than the yield strength	<50 % Rp: Negligible 50-70 % Rp: ±10% >70 % Rp.: Unknown	Ref. [8]

1) This figure is an estimate of the error when a 3-axial stress field (the stresses are varying with the hole depth) is evaluated as a uniform stress field. In this report the stresses are evaluated under the assumption of a non-uniform stress field. SP has found that evaluating the residual stresses with different methods (evaluated as uniform stress, using the power method or using the integral method) *can* give a larger scatter in the results. The actual uncertainty is therefore not fully known, but this figure indicates that the error can be large.

From *Table 2* it can be seen that the dominating error is the error when the non-uniform stresses are calculated. The contribution from the other errors are therefore small and the total uncertainty in the calculated stress values will be less than 20 %.

10 Results

Raw data as measured strains are given in *Appendix 2*

The calculated residual stresses are presented as max / min principal stresses in *Appendix 3*.

The stresses are also expressed in local coordinate systems referring to the gages and in a global coordinate system referring to the insert tube in *Appendix 4*.

SP Technical Research Institute of Sweden
SP Structural and Solid Mechanics - Life and Reliability

Performed by

Gunnar Kjell

Examined by

Billy Alvarsson

Appendices

Appendix 1	Photographs of the test set-up (5 pages)
Appendix 2	Raw data (measured strains) (7 pages)
Appendix 3	Max / min principle stresses calculated by the Integral method (8 pages)
Appendix 4	Normal and shear stresses in a global coordinate system (9 pages))

References

[1] P. Dillström, L. Alverlind, M. Andersson, 2010. "Framtagning av acceptanskriterier samt skadetålighetsanalyser av segjärnsinsatsen". SKB R-10-11, Svensk Kärnbränslehantering AB

[2] M. Wihed "Materialprovning av segjärnsinsats I56". *SKBdoc1094763,* Swerea SweCast AB, 2007.

[3] ASTM E 387-08 Standard Test method for Determining Residual Stresses by the Hole- Drilling Strain-Gage Method, 2008

[4] Technical Note TN-503-6, Measurement of Residual Stresses by the Hole-Drilling Strain Gage Method, Vishay Measurement Group, 2007.

[5] G.S. Schajer. "Measurement of Non-Uniform Residual Stresses Using the Hole-Drilling Method. *Journal of Engineering Materials and Technology*, Vol.110, No.4, 1988. "Part I Stress Calculation Procedures," pp.338-343, "Part II Practical Application of the Integral Method," pp 344-349.

[6] G.S. Schajer "H-Drill – Hole-Drilling Residual Stress Calculation Program" Ver 3.10 User guide, 2007

[7] PV Grant, PD Lord, PS Whitehead. “The measurement of residual stresses by the incremental hole drilling technique, measurement good practice guide 53”. National Physical Laboratory UK, 2002.

[8] R. Oettel “The Determination of Uncertainties in residual Stress Measurement (Using the hole drilling technique)”. *Manual of Codes of Practice for determination of uncertainties in mechanical tests on metallic material*. Project UNCERT, EU Contract SMT4-CT97-2165, Standards Measurement & Testing Programme, ISBN 0 946754 41 1, Issue 1, September 2000.

[9] “DHD residual stress measurements within the cast iron insert of a radioactive waste canister - report No R11-001”, SKBDoc 1321056, version 2.0

Appendix 1

Photographs of the test set-up

Figure A1:1 The sample lying on the packing pallets in the SP laboratory before the start of the measurement.

Figure A1:2 The marking on the sample.

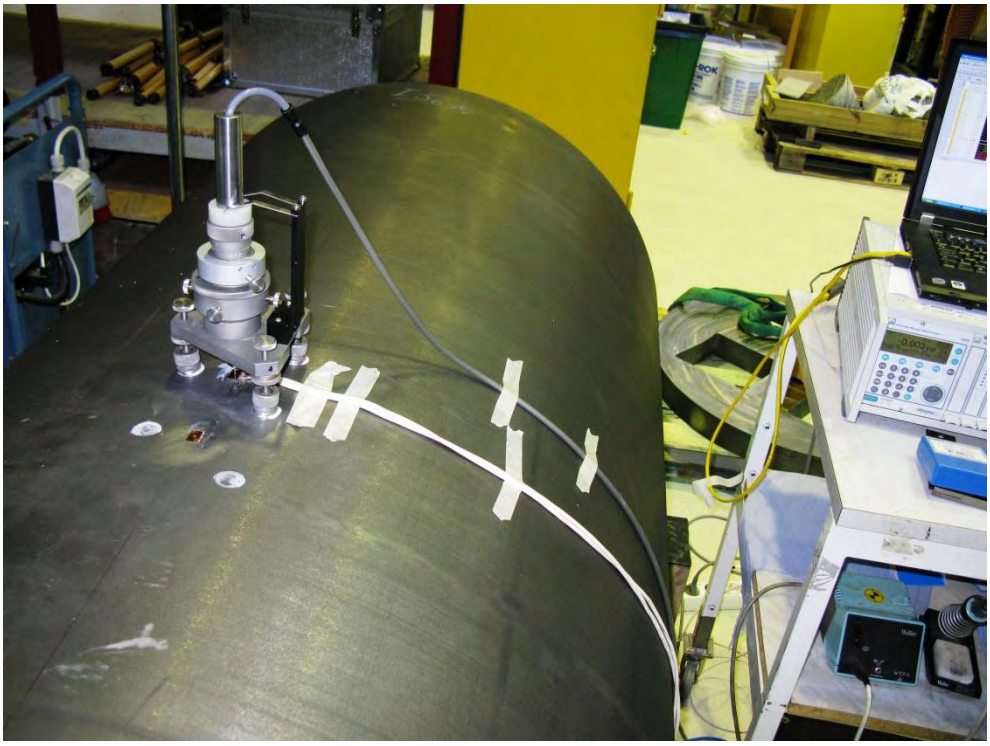

Figure A1:3 The hole drilling rig cemented to the sample.

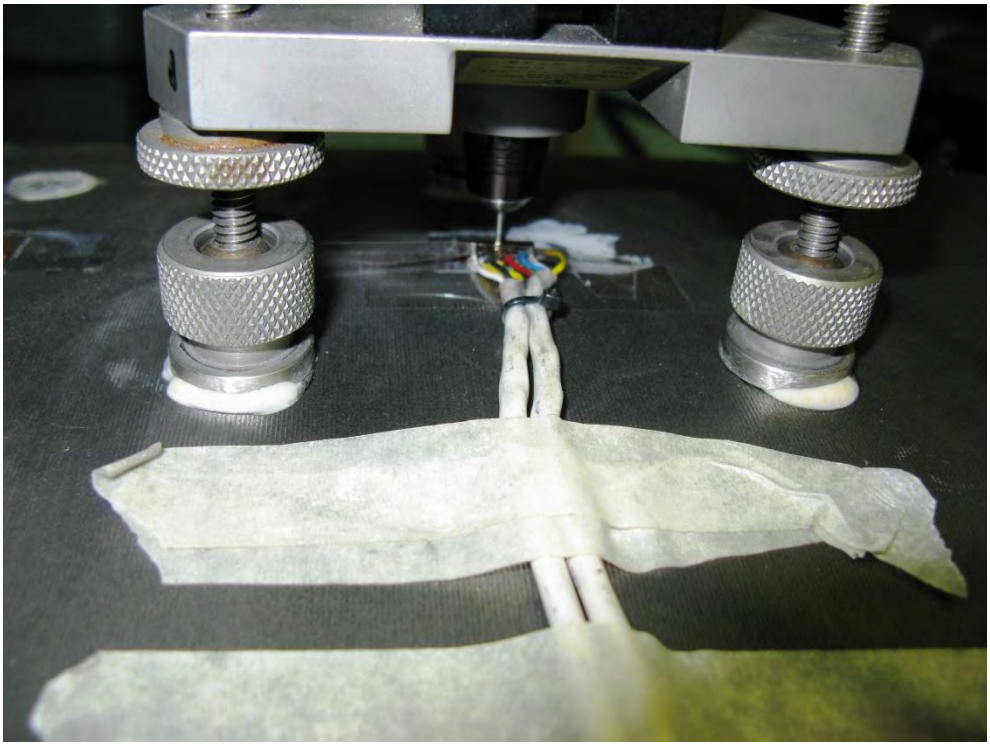

Figure A1:4 A second photograph showing the hole drilling rig cemented to the sample.

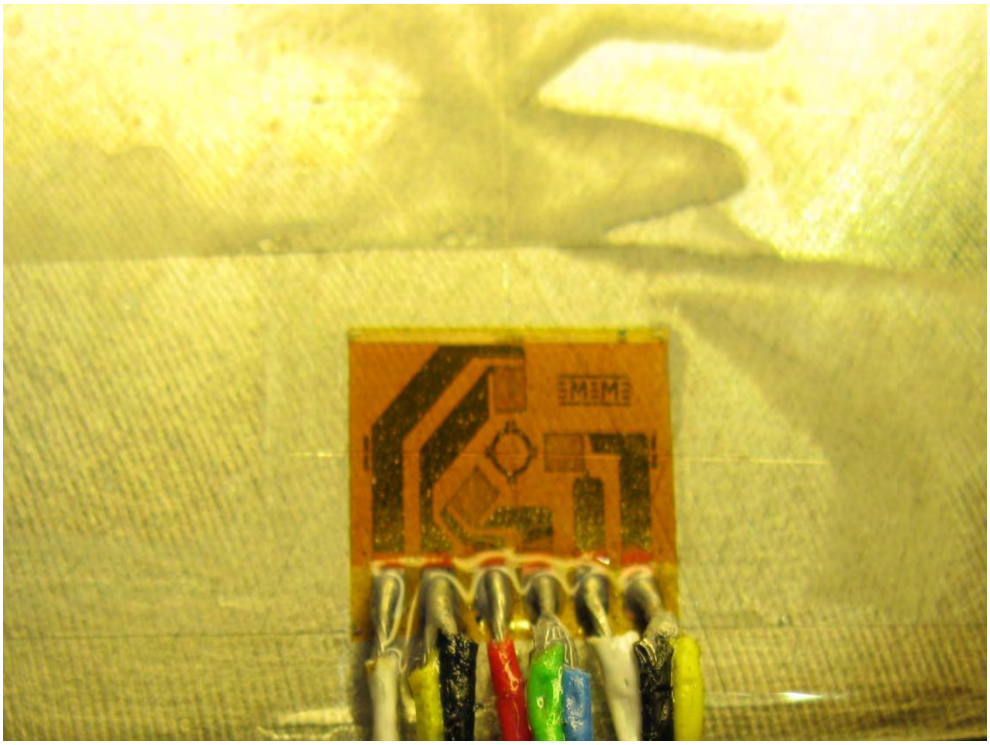

Figure A1:5 The 062UL strain gage bonded to the sample just before the drilling.

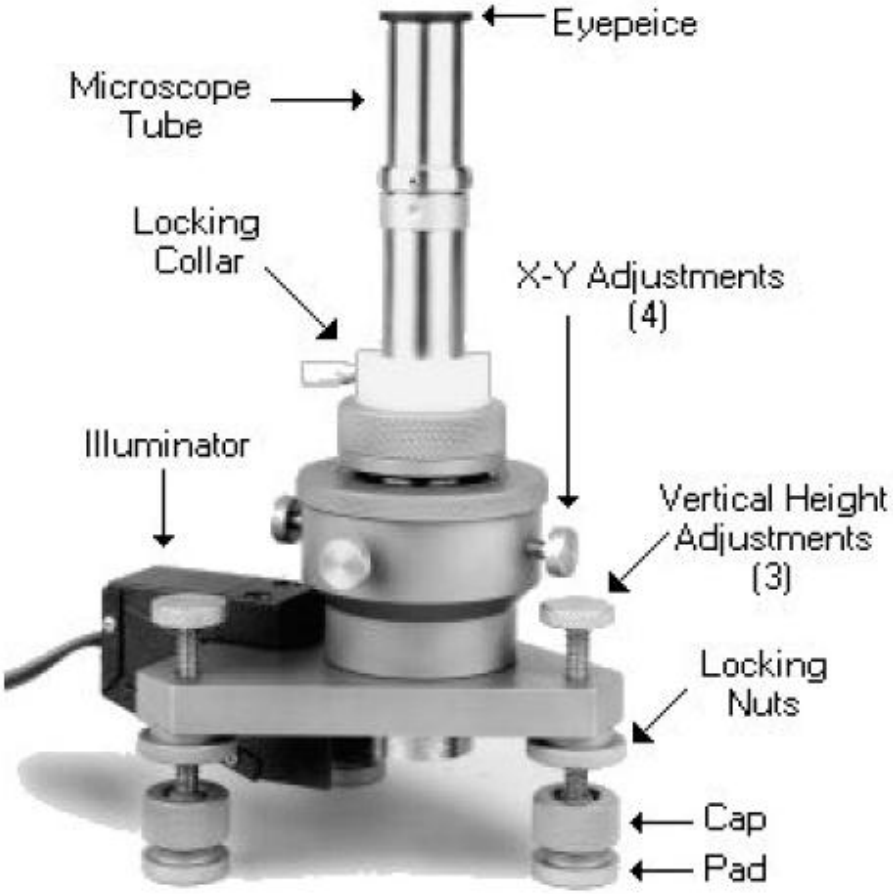

Figure A1:6 A picture of the milling guide supplied by the manufacture. A microscope is inserted in the milling guide so the guide can by the X-Y adjusting screws positioned over the centre of the gage.

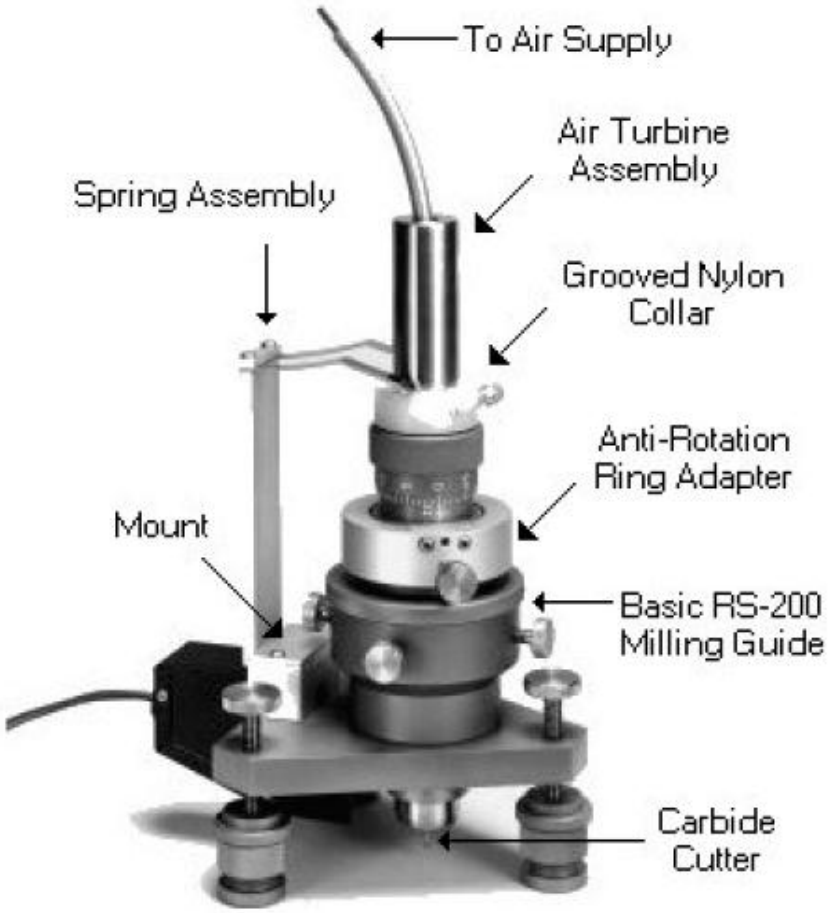

Figure A1:7 A picture of the milling guide supplied by the manufacture. A high speed air turbine is mounted in the guide.

Appendix 2

Raw data (measured strains)

This appendix contains raw data from the measurements. For each measuring point the data are listed in a table and plotted as a graph.

Table 1: Figures with raw data from the measurements on the sample

Measuring point	Figure	Measuring point	Figure	Measuring point	Figure
BWRinsats1	Fig: A2:1	BWRinsats2	Fig: A2:2	BWRinsats3	Fig: A3:2
BWRinsats4	Fig: A2:4	BWRinsats5	Fig: A2:5	BWRinsats5a	Fig: A2:6
BWRinsats5b	Fig: A2:7	BWRinsats6	Fig: A2:8	BWRinsats7	Fig: A2:9
BWRinsats8	Fig: A2:10	BWRinsats9	Fig: A2:11	---	---

During the drilling at location 5 the reading from the strain gages suddenly increased with a large step. This was probably caused by bending from the cutter when it hit some hard inclusion in the material. The measuring was aborted and a new measurement to the left was done. Even this measuring was disturbed and a third measuring was done to the right of the original point 5. Also the measurements from point 6 was disturbed and had to be aborted before the hole depth 1.91mm was reached. However, the measured values at location 5, 5a and 5b presented in this report are measured before the steps occurred and are therefore correct.

Appendix 2

Depth mm	Gage 1 µm/m	Gage 2 µm/m	Gage 3 µm/m
0.00	-2	-1	2
0.13	3	8	17
0.25	11	21	37
0.38	0	23	50
0.51	29	53	79
0.64	53	78	100
0.76	73	98	115
0.89	92	113	126
1.02	108	125	136
1.14	119	134	140
1.27	129	140	145
1.40	136	144	147
1.52	139	146	148
1.65	143	149	149
1.78	146	150	149
1.91	148	150	148

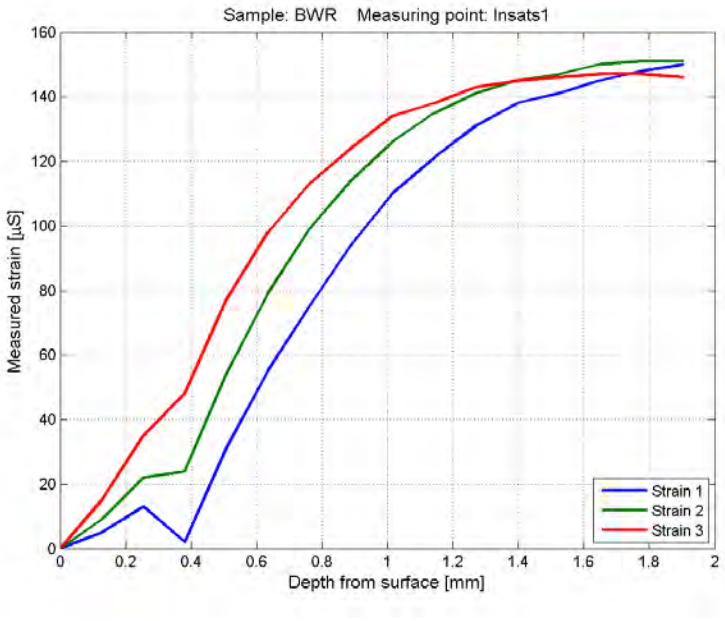

Figure A2:1 Raw data from measurement point BWRinsats1. There is a rather small jump in the measured strains between the readings at 0.25mm and 0.38mm. The jump is probably caused by bending from the cutter when it hit some hard inclusion in the material.

Depth mm	Gage 1 µm/m	Gage 2 µm/m	Gage 3 µm/m
0.00	1	0	0
0.13	6	10	22
0.25	15	23	48
0.38	30	41	79
0.51	47	57	102
0.64	68	76	123
0.76	89	92	137
0.89	107	106	145
1.02	121	115	150
1.14	130	121	152
1.27	137	125	153
1.40	140	127	151
1.52	144	129	151
1.65	147	129	149
1.78	148	129	147
1.91	149	129	145

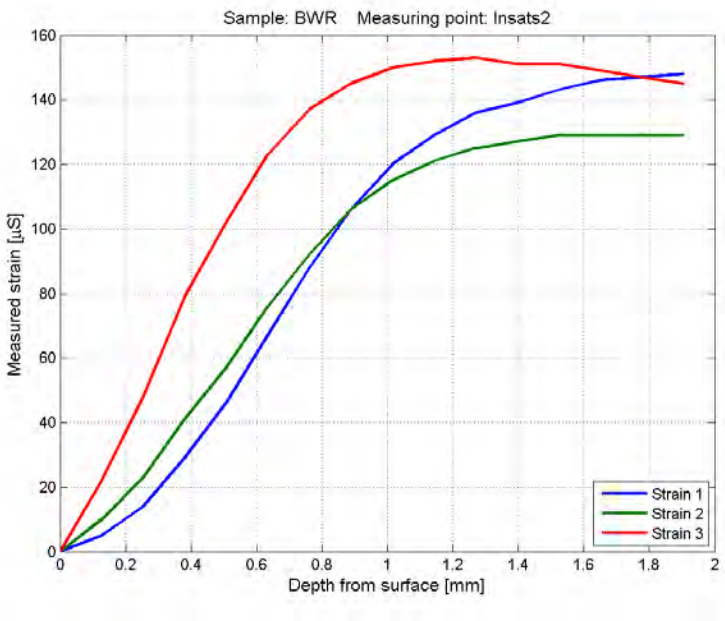

Figure A2:2 Raw data from measurement point BWRinsats2

Depth mm	Gage 1 µm/m	Gage 2 µm/m	Gage 3 µm/m
0.00	1	0	0
0.13	1	6	16
0.25	8	20	39
0.38	20	36	66
0.51	37	54	91
0.64	56	70	108
0.76	76	84	121
0.89	92	94	127
1.02	106	102	131
1.14	115	107	133
1.27	123	112	135
1.40	127	114	134
1.52	129	115	133
1.65	131	115	132
1.78	132	115	130
1.91	132	115	128

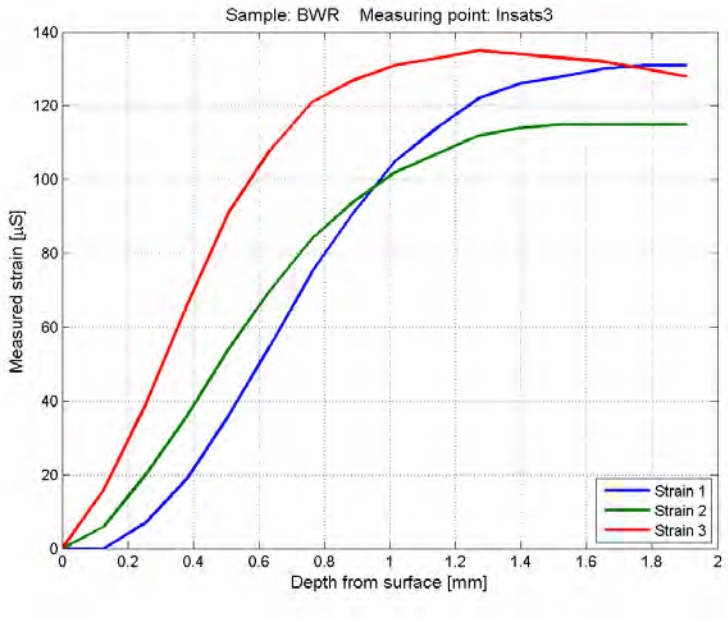

Figure A2:3 Raw data from measurement point BWRinsats3

Depth mm	Gage 1 µm/m	Gage 2 µm/m	Gage 3 µm/m
0.00	0	0	0
0.13	3	7	16
0.25	9	20	37
0.38	23	38	62
0.51	41	55	85
0.64	59	70	104
0.76	74	83	121
0.89	87	93	134
1.02	97	100	144
1.14	103	105	150
1.27	107	107	154
1.40	110	108	157
1.52	110	108	157
1.65	111	108	158
1.78	111	107	158
1.91	110	105	157

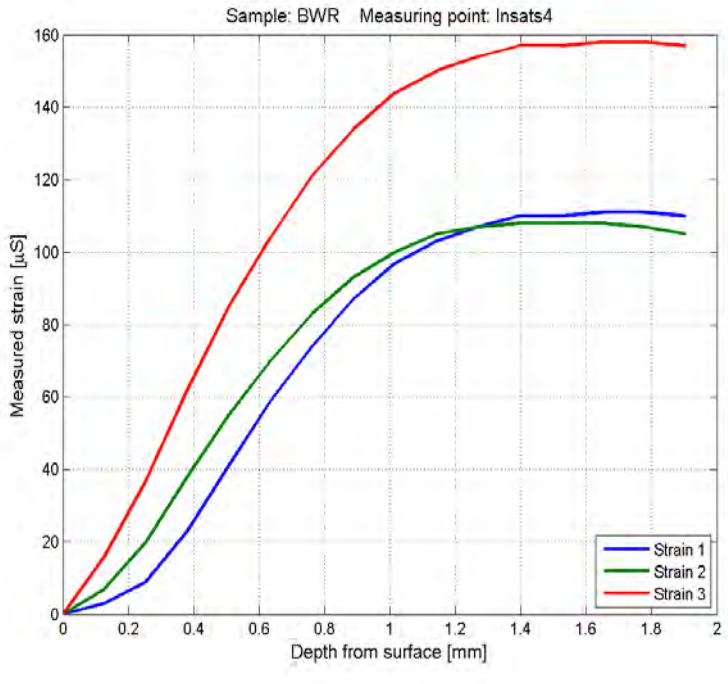

Figure A2:4 Raw data from measurement point BWRinsats4

Depth mm	Gage 1 µm/m	Gage 2 µm/m	Gage 3 µm/m
0.00	0	-1	0
0.13	3	6	18
0.25	10	17	39
0.38	22	32	65
0.51	40	48	87
0.64	61	65	108
0.76	80	77	122

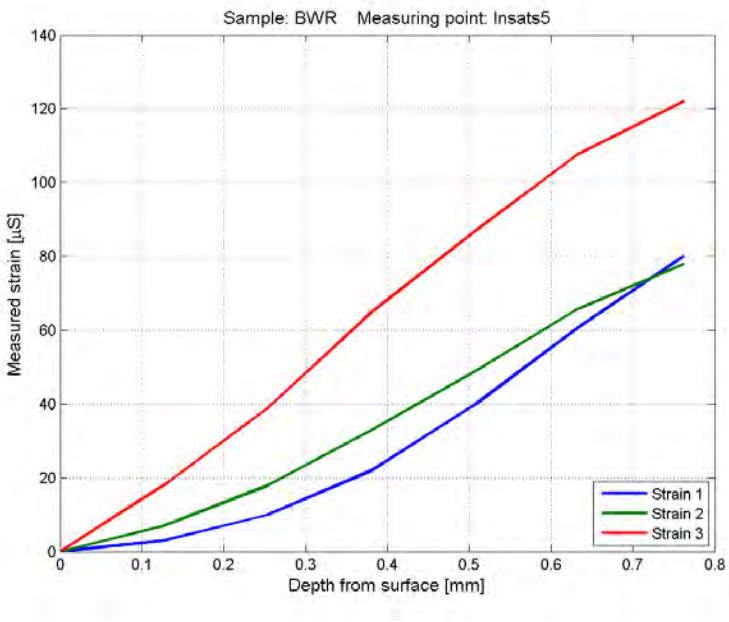

Figure A2:5 Raw data from measurement point BWRinsats5

Depth mm	Gage 1 µm/m	Gage 2 µm/m	Gage 3 µm/m
0.00	2	0	0
0.13	12	14	26
0.25	23	29	50
0.38	35	42	72
0.51	52	54	93

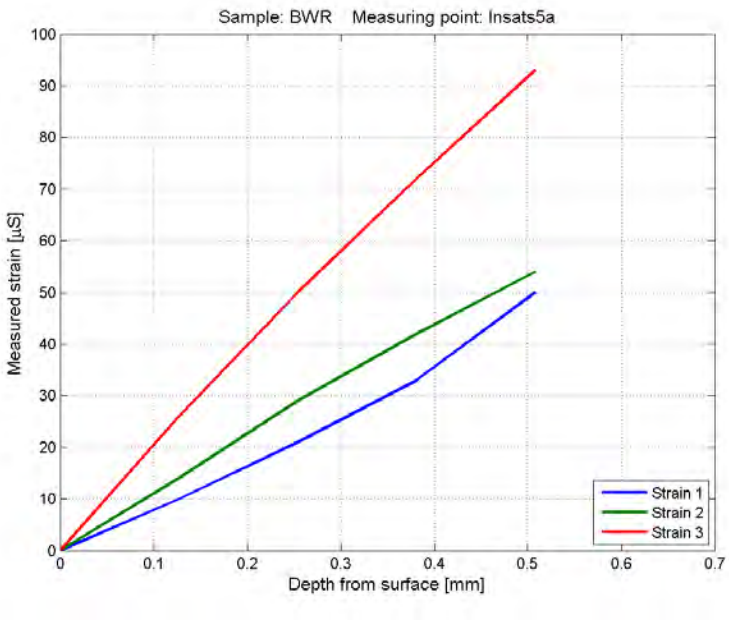

Figure A2:6 Raw data from measurement point BWRinsats5a

Depth mm	Gage 1 µm/m	Gage 2 µm/m	Gage 3 µm/m
0.00	0	-1	-1
0.13	5	10	19
0.25	15	25	45
0.38	28	40	74
0.51	43	54	96
0.64	62	69	114
0.76	80	83	130
0.89	97	99	144
1.02	110	108	153

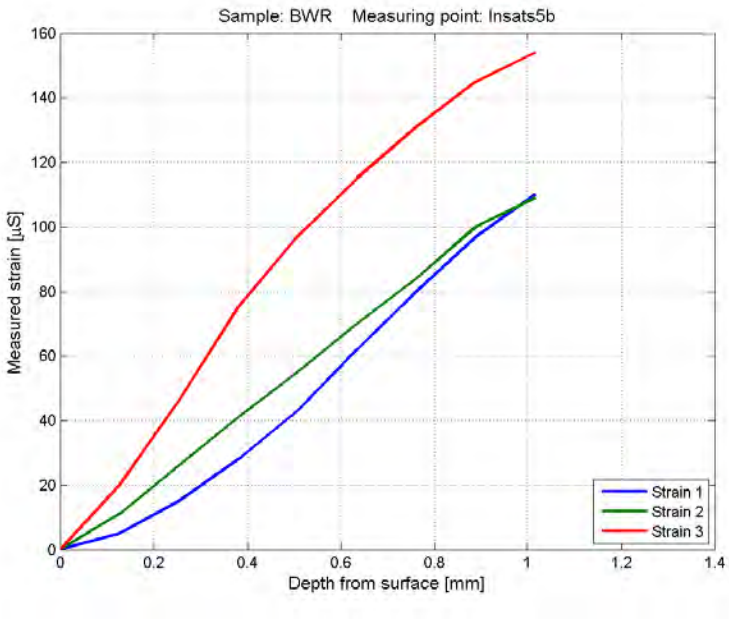

Figure A2:7 Raw data from measurement point BWRinsats5b

Depth mm	Gage 1 µm/m	Gage 2 µm/m	Gage 3 µm/m
0.00	0	-1	0
0.13	0	5	16
0.25	12	17	42
0.38	23	27	63
0.51	39	37	81
0.64	57	51	99
0.76	74	62	115
0.89	91	73	129

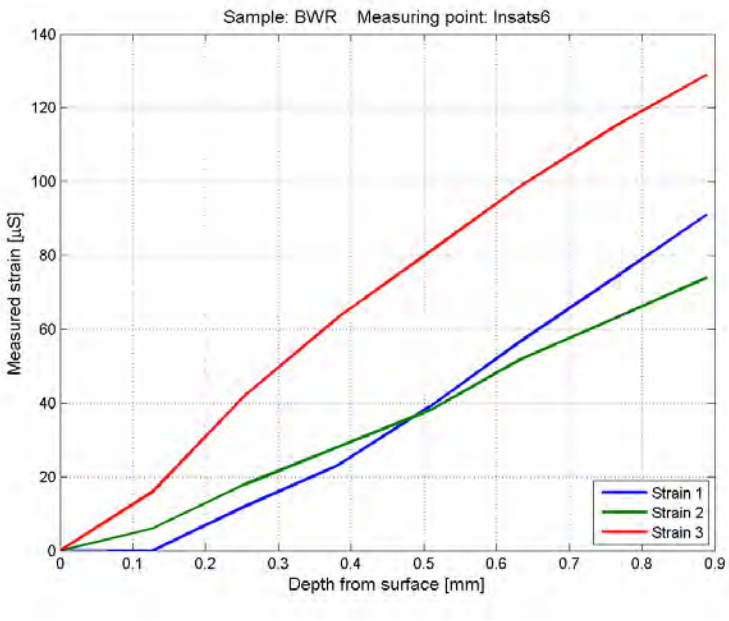

Figure A2:8 Raw data from measurement point BWRinsats6

Depth mm	Gage 1 µm/m	Gage 2 µm/m	Gage 3 µm/m
0.00	0	0	0
0.13	4	13	27
0.25	14	33	56
0.38	25	49	77
0.51	38	61	95
0.64	52	75	112
0.76	64	85	124
0.89	73	92	134
1.02	84	101	143
1.14	91	106	149
1.27	92	106	150
1.40	94	106	151
1.52	98	108	155

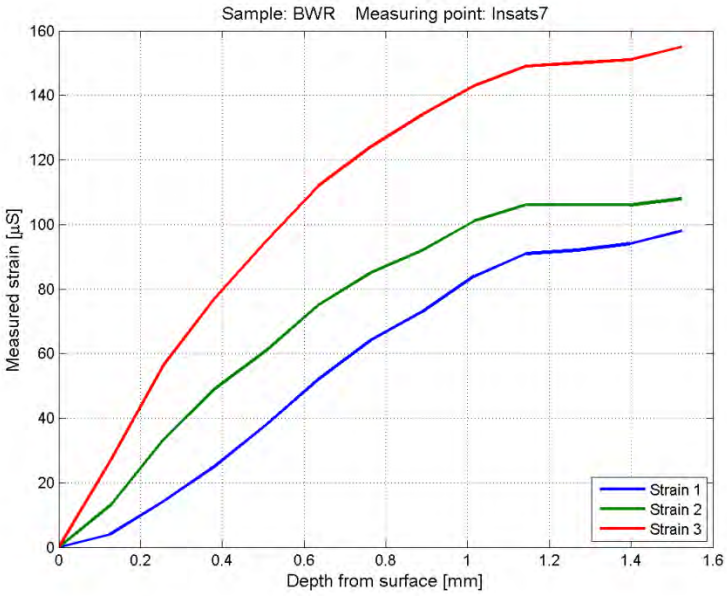

Figure A2:9 Raw data from measurement point BWRinsats7

Depth mm	Gage 1 µm/m	Gage 2 µm/m	Gage 3 µm/m
0.00	-1	0	0
0.13	3	10	24
0.25	13	28	54
0.38	24	42	72
0.51	38	56	89
0.64	51	71	104
0.76	66	85	117
0.89	81	98	134
1.02	92	107	142
1.14	103	114	151
1.27	107	117	154
1.40	110	120	157
1.52	110	119	157
1.65	112	119	156
1.78	111	118	155
1.91	111	117	154

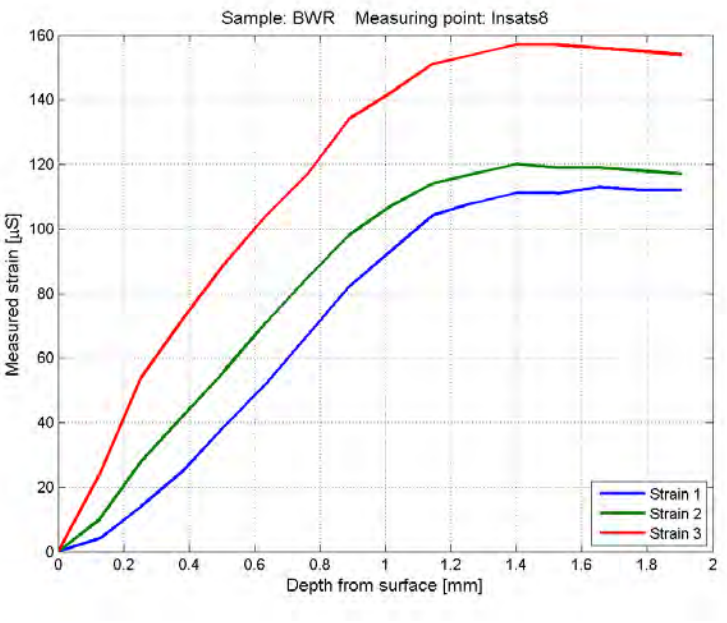

Figure A2:10 Raw data from measurement point BWRinsats8

Appendix 2

Depth mm	Gage 1 µm/m	Gage 2 µm/m	Gage 3 µm/m
0.00	0	-1	0
0.13	4	13	25
0.25	15	30	53
0.38	27	46	74
0.51	41	60	92
0.64	55	75	109
0.76	68	87	123
0.89	82	100	138
1.02	97	113	152
1.14	107	121	161
1.27	110	124	164
1.40	113	125	166
1.52	114	126	167
1.65	115	125	167
1.78	115	125	167
1.91	113	122	165

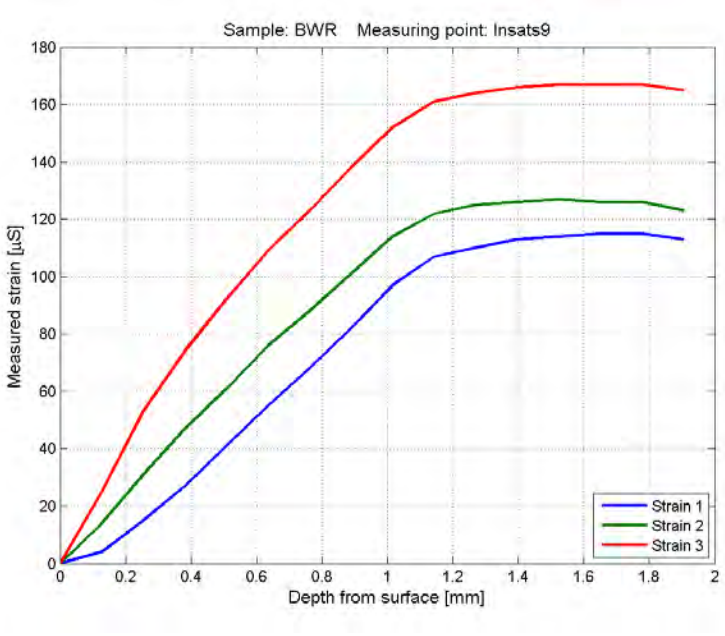

Figure A2:11 Raw data from measurement point BWRinsats9

Max / min principal stresses calculated by the Integral method

This appendix contains max / min principal stresses [1] calculated by the *Integral method*.

For each measuring point one table and two graphs are supplied. All calculated stresses and angles are shown in the table. The first graph shows the maximum and minimum principal stress and the second graph shows the orientation of the principal stress direction (the clockwise angle between the Strain Gage 1 and the axis of the maximum principal stress), see Figure A3:1.

Table 1: Figures with max / min principal stresses in the BWR sample

Measuring point	Figure	Measuring point	Figure	Measuring point	Figure
BWRinsats1	Fig: A3:2	BWRinsats2	Fig: A3:3	BWRinsats3	Fig: A3:4
BWRinsats4	Fig: A3:5	BWRinsats5	Fig: A3:6	BWRinsats5a	Fig: A3:7
BWRinsats5b	Fig: A3:8	BWRinsats6	Fig: A3:9	BWRinsats7	Fig: A3:10
BWRinsats8	Fig: A3:11	BWRinsats9	Fig: A3:12	---	---

During the drilling at location 5 the reading from the strain gages suddenly increased with a large step. This was probably caused by bending from the cutter when it hit some hard inclusion in the material. The measuring was aborted and a new measurement to the left was done. Even this measuring was disturbed and a third measuring was done to the right of the original point 5. Also the measurements from point 6 was disturbed and had to be aborted before the hole depth 1.91mm was reached. However, all measured values presented in this report are measured before the steps occurred and are therefore correct.

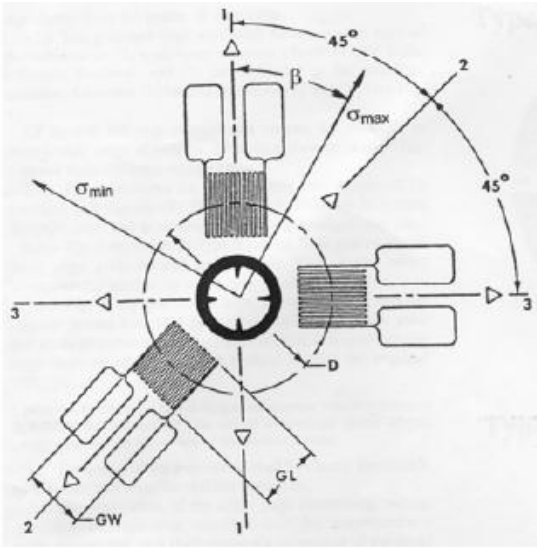

Figure A3:1 A sketch showing the orientations of the three strain gages and the definition of the angle β

[1] At every point in a stressed body there are at least one rectangular coordinate system where the corresponding sheer stresses are zero. The corresponding stresses are called principal stresses. On a surface where the normal stress is zero there are two such principal stresses.

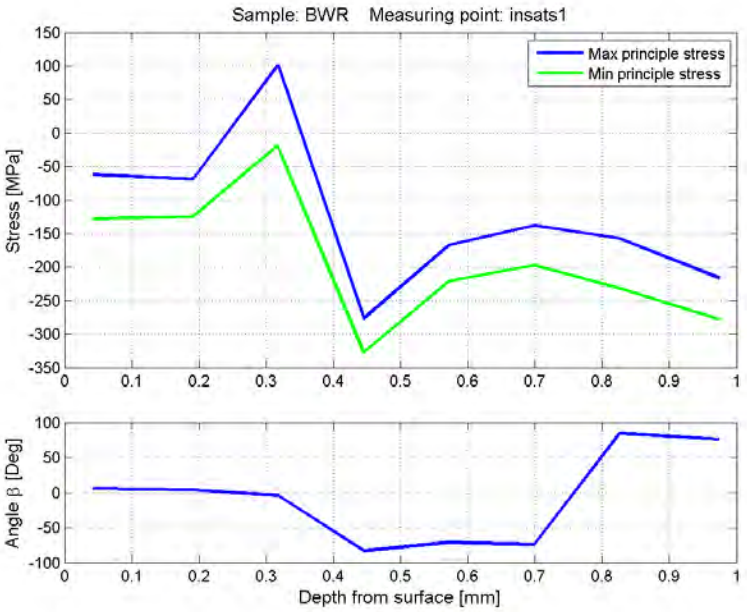

Depth mm	σ_{Max} MPa	σ_{Min} MPa	β Deg
0.04	-62	-128	6
0.19	-69	-125	4
0.32	101	-19	-4
0.45	-277	-327	-83
0.57	-167	-221	-71
0.70	-138	-197	-74
0.83	-157	-232	85
0.97	-216	-278	76

Figure A3:2 Principal stresses calculated for the measuring point insats1 on the sample. As can be seen from the raw data (Figure A2:1 in Appendix 2) there was a relative small jump in the measured strains. The tension stresses at the depth 0.32 mm are caused by the disturbances caused by this jump and are therefore not reliable. For the other shaded stresses the von Mises effective stress is larger than 70% of the yield stress and therefore they are not reliable..

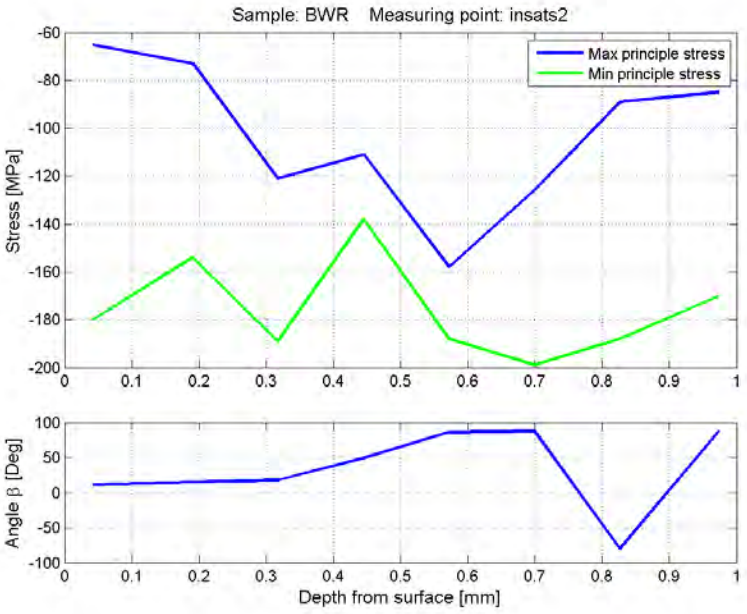

Depth mm	σ_{Max} MPa	σ_{Min} MPa	β Deg
0.04	-65	-180	11
0.19	-73	-154	15
0.32	-121	-189	18
0.45	-111	-138	49
0.57	-158	-188	86
0.70	-126	-199	88
0.83	-89	-188	-80
0.97	-85	-170	88

Figure A3:3 Principal stresses calculated for the measuring point insat2 on the sample.

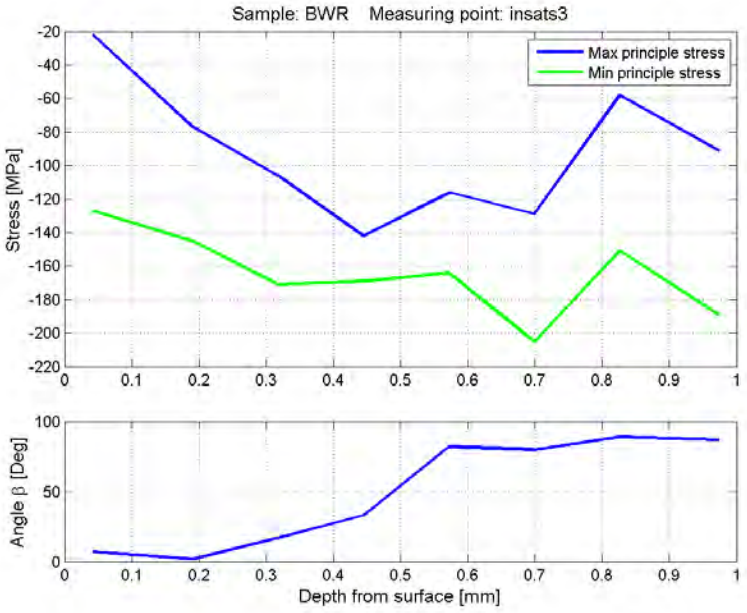

Depth mm	σ_{Max} MPa	σ_{Min} MPa	β Deg
0.04	-22	-127	7
0.19	-77	-145	2
0.32	-106	-171	17
0.45	-142	-169	33
0.57	-116	-164	82
0.70	-129	-205	80
0.83	-58	-151	89
0.97	-91	-189	87

Figure A3:4 Principal stresses calculated for the measuring point *insats3* on the sample.

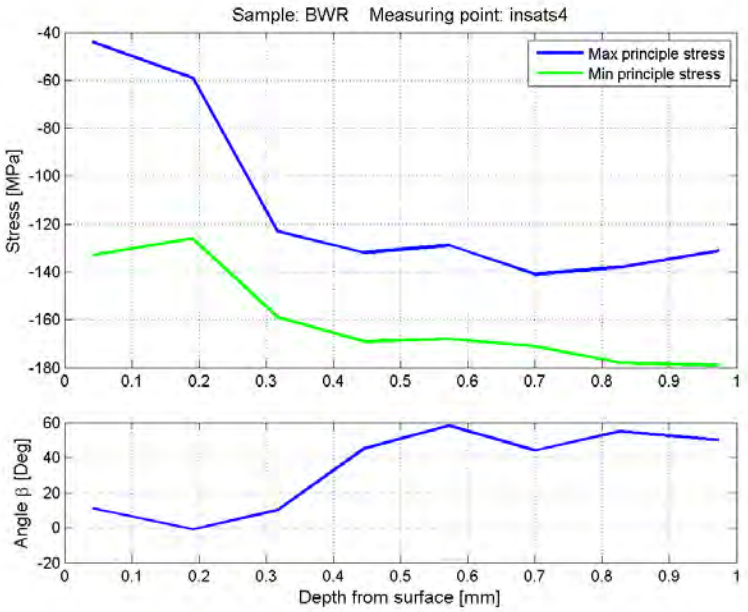

Depth mm	σ_{Max} MPa	σ_{Min} MPa	β Deg
0.04	-44	-133	11
0.19	-59	-126	-1
0.32	-123	-159	10
0.45	-132	-169	45
0.57	-129	-168	58
0.70	-141	-171	44
0.83	-138	-178	55
0.97	-131	-179	50

Figure A3:5 Principal stresses calculated for the measuring point *insats4* on the sample

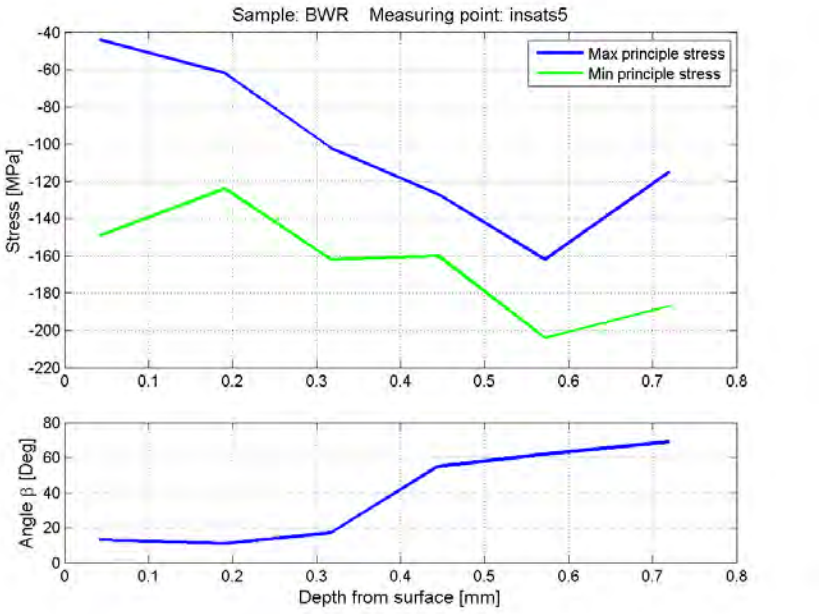

Depth mm	σ_{Max} MPa	σ_{Min} MPa	β Deg
0.04	-44	-149	13
0.19	-62	-124	11
0.32	-102	-162	17
0.45	-127	-160	55
0.57	-162	-204	62
0.72	-115	-187	69

Figure A3:6 Principal stresses calculated for the measuring point *insats5* on the sample.

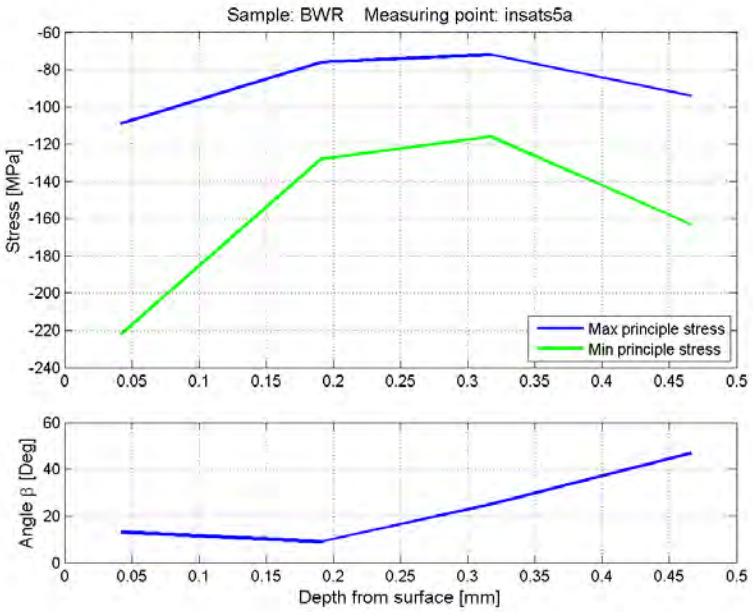

Depth mm	σ_{Max} MPa	σ_{Min} MPa	β Deg
0.04	-109	-222	13
0.19	-76	-128	9
0.32	-72	-116	25
0.47	-94	-163	47

Figure A3:7 Principal stresses calculated for the measuring point *insats5a* on the sample.

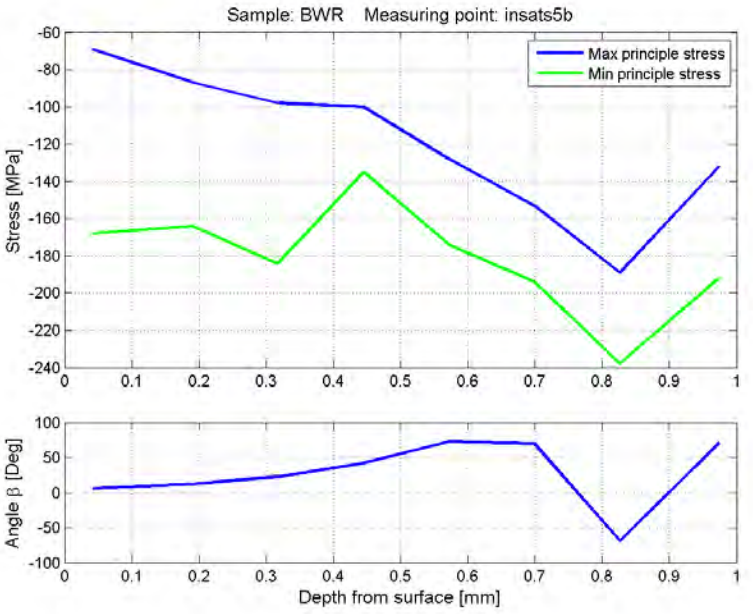

Depth mm	σ_{Max} MPa	σ_{Min} MPa	β Deg
0.04	-69	-168	6
0.19	-87	-164	12
0.32	-98	-184	23
0.45	-100	-135	42
0.57	-128	-174	73
0.70	-153	-194	70
0.83	-189	-238	-69
0.97	-132	-192	71

Figure A3:8 Principal stresses calculated for the measuring point *insats5b* on the sample. For the shaded stresses the von Mises effective stress is larger than 70% of the yield stress and therefore they are not reliable.

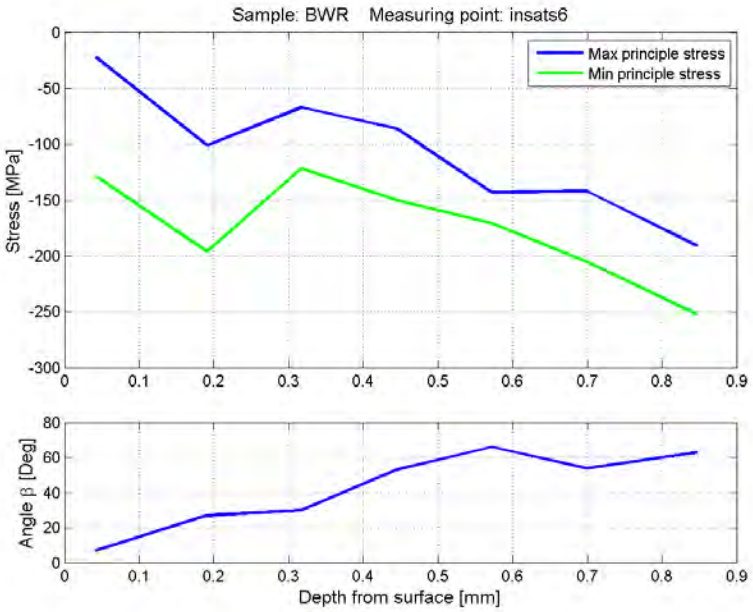

Depth mm	σ_{Max} MPa	σ_{Min} MPa	β Deg
0.04	-22	-129	7
0.19	-101	-196	27
0.32	-67	-122	30
0.45	-86	-150	53
0.57	-143	-171	66
0.70	-142	-205	54
0,85	-191	-252	63

Figure A3:9 Principal stresses calculated for the measuring point *insats6* on the sample. For the shaded stresses the von Mises effective stress is larger than 70% of the yield stress and therefore they are not reliable.

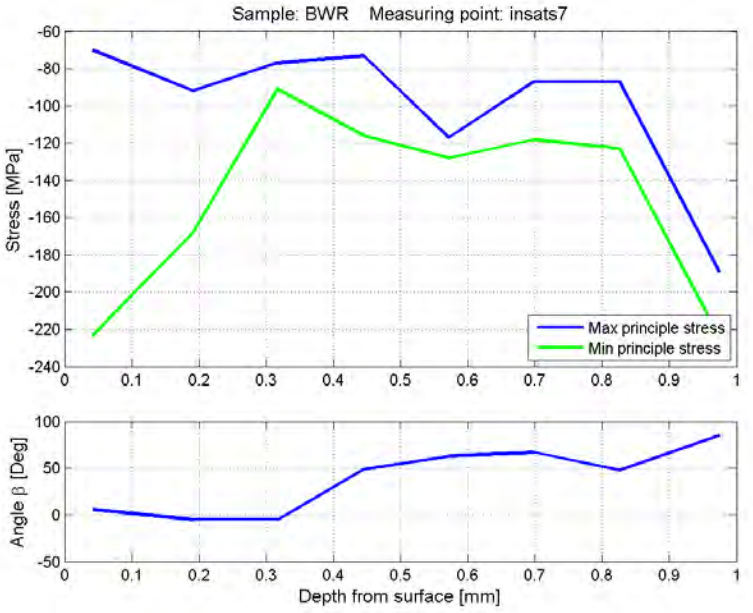

Depth mm	σ_{Max} MPa	σ_{Min} MPa	β Deg
0.04	-70	-223	6
0.19	-92	-168	-5
0.32	-77	-91	-5
0.45	-73	-116	49
0.57	-117	-128	63
0.70	-87	-118	67
0.83	-87	-123	48
0.97	-189	-224	85

Figure A3:10 Principal stresses calculated for the measuring point *insats7* on the sample. For the shaded stresses the von Mises effective stress is larger than 70% of the yield stress and therefore they are not reliable.

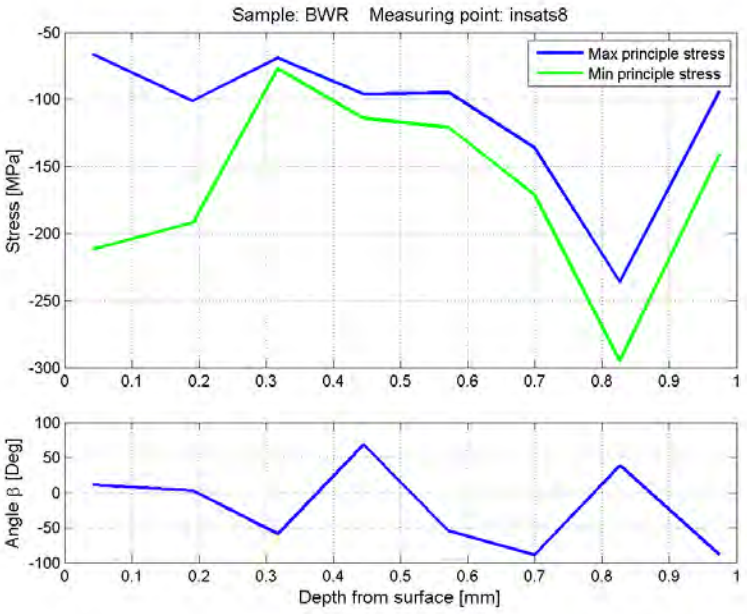

Depth mm	σ_{Max} MPa	σ_{Min} MPa	β Deg
0.04	-66	-212	11
0.19	-101	-192	3
0.32	-69	-77	-59
0.45	-96	-114	69
0.57	-95	-121	-55
0.70	-136	-171	-89
0.83	-236	-295	39
0.97	-94	-141	-88

Figure A3:11 Principal stresses calculated for the measuring point *insats8* on the sample. For the shaded stresses the von Mises effective stress is larger than 70% of the yield stress and therefore they are not reliable.

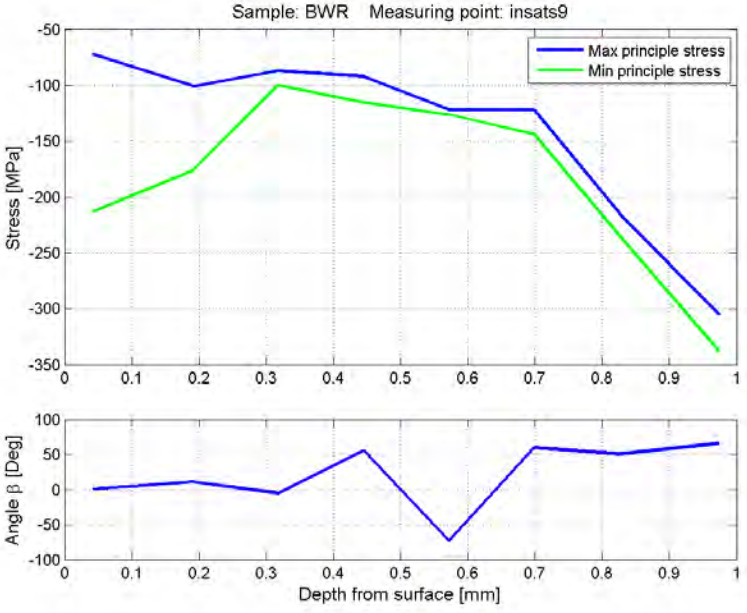

Depth mm	σ_{Max} MPa	σ_{Min} MPa	β Deg
0.04	-72	-213	1
0.19	-101	-176	11
0.32	-87	-100	-5
0.45	-92	-115	56
0.57	-122	-126	-73
0.70	-122	-144	60
0.83	-215	-235	51
0.97	-305	-338	66

Figure A3:12 Principal stresses calculated for the measuring point *insats9* on the sample. For the shaded stresses the von Mises effective stress is larger than 70% of the yield stress and therefore they are not reliable.

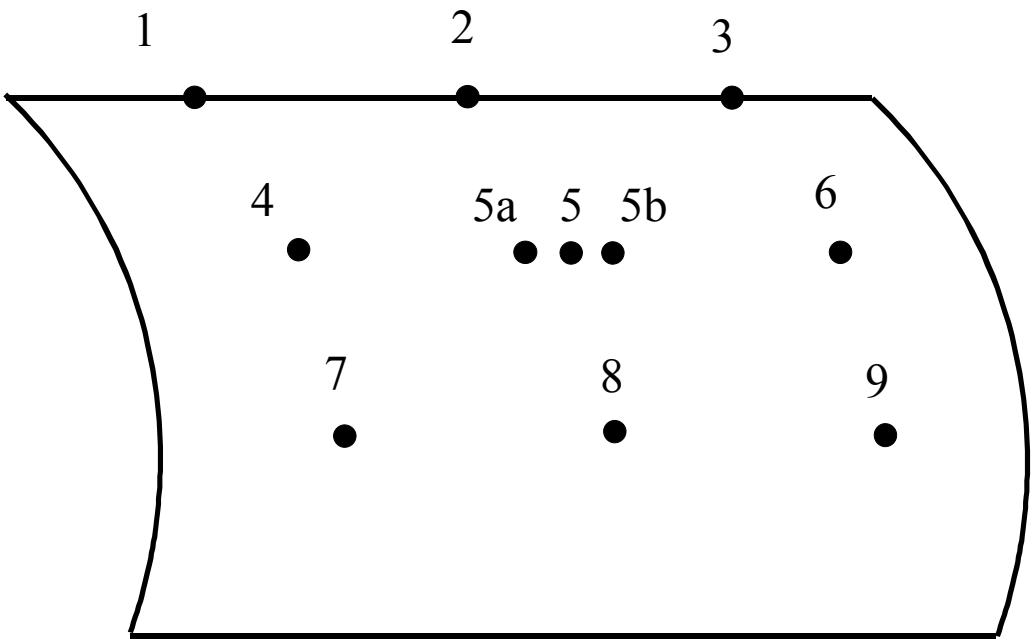

Measuring point	Max stress	Measuring point	Max stress	Measuring point	Max stress
BWRinsats1	101	BWRinsats2	-65	BWRinsats3	-22
BWRinsats4	-44	BWRinsats5	-44	BWRinsats5a	-72
BWRinsats5b	-69	BWRinsats6	-22	BWRinsats7	-70
BWRinsats8	-66	BWRinsats9	-72	---	

Figure A3:13 A summary of the results from the measurement. For each measurement point the maximum calculated stress (the minimum compressive stress) is given. The aim of this table is to give a quick view of the results and it will not replace the results given in the previous figures. The tension stresses at the location BWRinsats1 are not reliable; see the captions to *Figure A2.1* (in *Appendix 2*) and *Figure A3:2*(in this appendix). According to the main report the uncertainty in the reported values is 15-20%

Appendix 4

Normal and shear stresses in a global coordinate system

In *Appendix 3* the principle stresses are calculated from the measured strains and calculated by the integral method In this appendix the stresses are expressed in the local coordinate system referring to the gages and in a global coordinate system referring to the directions in the insert tube.

The gages in the rosette are named Strain gage 1, Strain gage 2 and Strain gage 3 according to Figure A4: 1

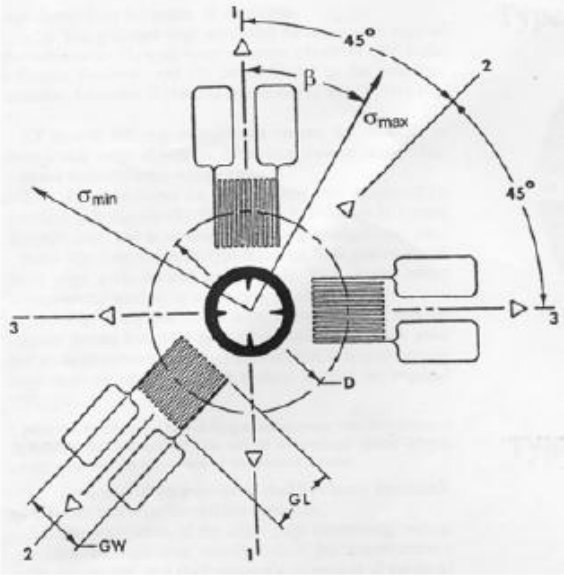

Figure A4: 1 A sketch showing the orientations of the three strain gages and the definition of the angle β.

In this report the X-direction is the direction of Strain gage 1 and the Y-direction is the direction of Strain gage 3.The angle β is the clockwise angle between Strain gage 1 and the maximum principle stress. With this directions the stresses in the local coordinate system can be calculated from Figure A4: 2

For each measuring point one table and one graph are supplied. All calculated stresses are shown in the table.

Appendix 4

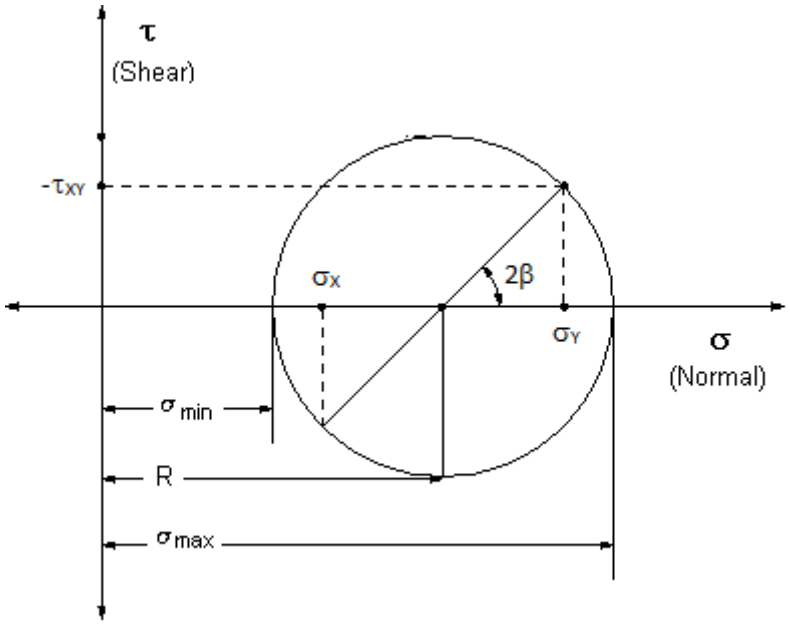

Figure A4: 2 Mohrs circle, with the directions and angles defined in Figure A4: 2. Mohrs circle is used for calculating the stresses in the local coordinate system.

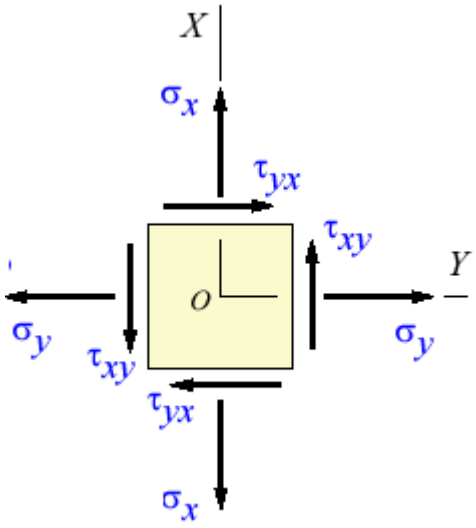

Figure A4: 3 Definition of the directions for the local stresses.

As global coordinate system for the insert tube, cylindrical coordinates (r,θ,z) are used, see Figure A4: 4.

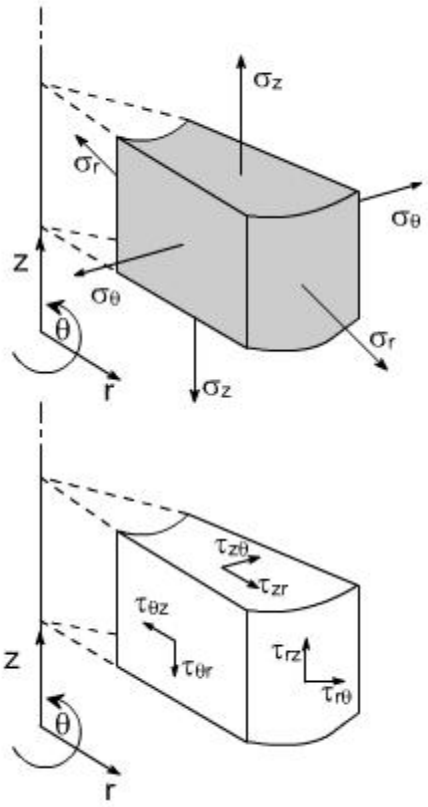

Figure A4: 4 The global coordinate referring to the insert tube, The hoop direction is named θ, the axial z and the radial r.

At the measurements done at SP, all gages were bonded so that the X-direction corresponds to the θ-direction (hoop) and the Y-direction to the z-direction (axial).

Table A4: 1: Figures local / global stresses in the BWR sample

Measuring point	Figure	Measuring point	Figure	Measuring point	Figure
BWRinsats1	Fig: A4:5	BWRinsats2	Fig: A4:6	BWRinsats3	Fig: A4:7
BWRinsats4	Fig: A4:8	BWRinsats5	Fig: A4:9	BWRinsats5a	Fig: A4:10
BWRinsats5b	Fig: A4:11	BWRinsats6	Fig: A4:12	BWRinsats7	Fig: A4:13
BWRinsats8	Fig: A4:14	BWRinsats9	Fig: A4:15	---	---

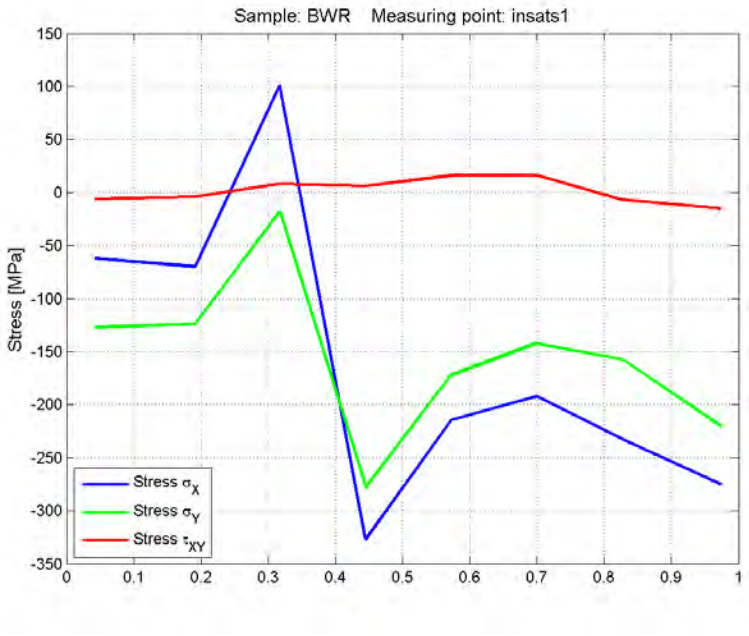

Depth mm	Hoop MPa	Axial MPa	Shear MPa	σ_e MPa
0.04	-62	-127	-6	109
0.19	-70	-124	-4	107
0.32	101	-18	8	111
0.45	-327	-278	6	305
0.57	-215	-172	16	197
0.70	-192	-142	16	172
0.83	-232	-157	-7	205
0.97	-275	-220	-15	251

Figure A4: 5 Stresses calculated for the measuring point insats1 on the sample. As can be seen from the raw data (Figure A2:1 in Appendix 2) there was a relative small jump in the measured strains. The tension stresses at the depth 0.32 mm are caused by the disturbances caused by this jump and are therefore not reliable. For the shaded stresses the von Mises effective stress is larger than 70% of the yield stress and therefore they are not reliable.

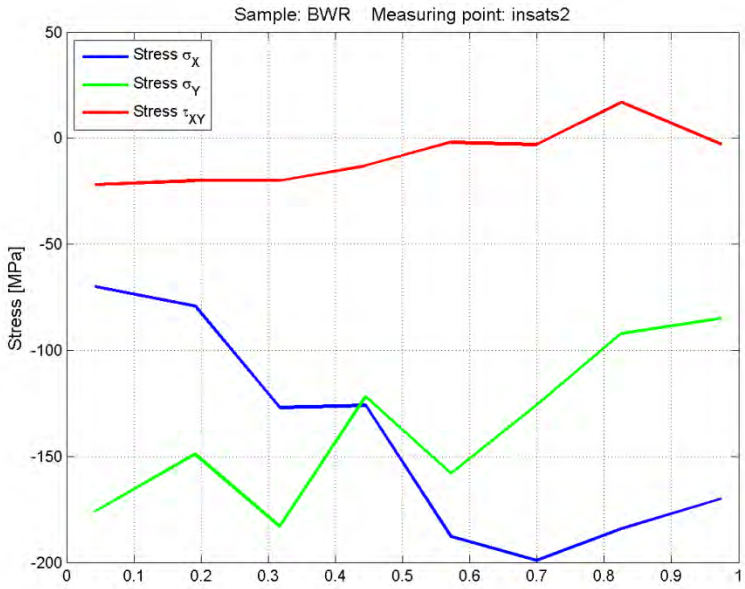

Depth mm	Hoop MPa	Axial MPa	Shear MPa	σ_e MPa
0.04	-70	-176	-22	153
0.19	-79	-149	-20	128
0.32	-127	-183	-20	162
0.45	-126	-122	-13	123
0.57	-188	-158	-2	174
0.70	-199	-126	-3	174
0.83	-184	-92	17	159
0.97	-170	-85	-3	147

Figure A4: 6 Stresses calculated for the measuring point insat2 on the sample.

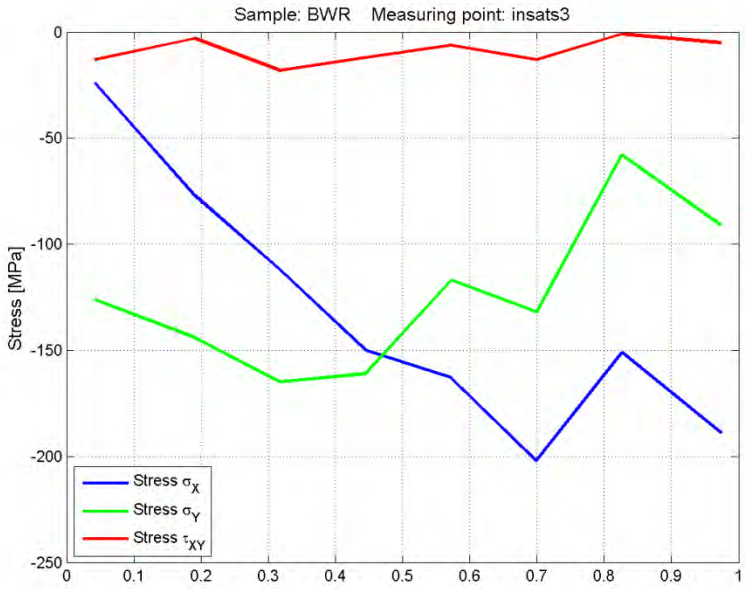

Depth mm	Hoop MPa	Axial MPa	Shear MPa	σ_e MPa
0.04	-24	-126	-13	115
0.19	-77	-144	-3	124
0.32	-112	-165	-18	145
0.45	-150	-161	-12	155
0.57	-163	-117	-6	145
0.70	-202	-132	-13	177
0.83	-151	-58	-1	131
0.97	-189	-91	-5	163

Figure A4: 7 Stresses calculated for the measuring point *insats3* on the sample.

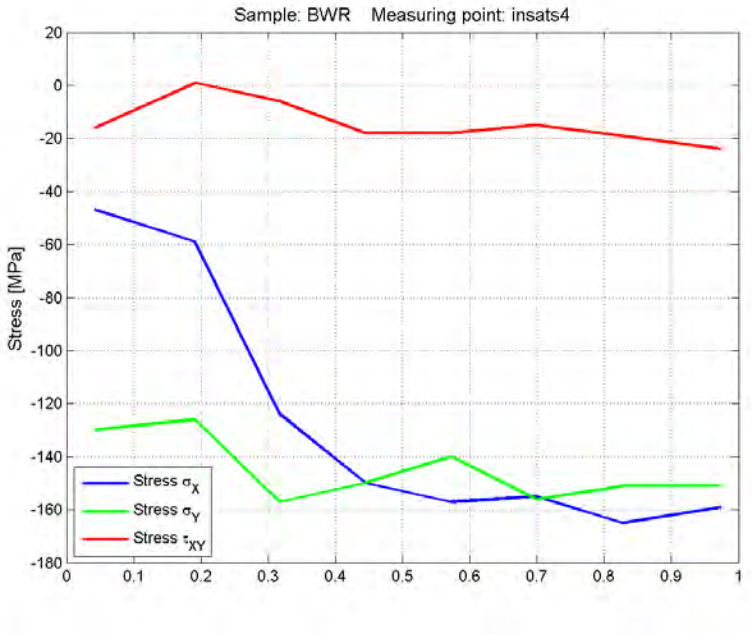

Depth mm	Hoop MPa	Axial MPa	Shear MPa	σ_e MPa
0.04	-47	-130	-16	113
0.19	-59	-126	1	109
0.32	-124	-157	-6	143
0.45	-150	-150	-18	149
0.57	-157	-140	-18	149
0.70	-155	-156	-15	155
0.83	-165	-151	-19	158
0.97	-159	-151	-24	154

Figure A4: 8 Stresses calculated for the measuring point *insats4* on the sample.

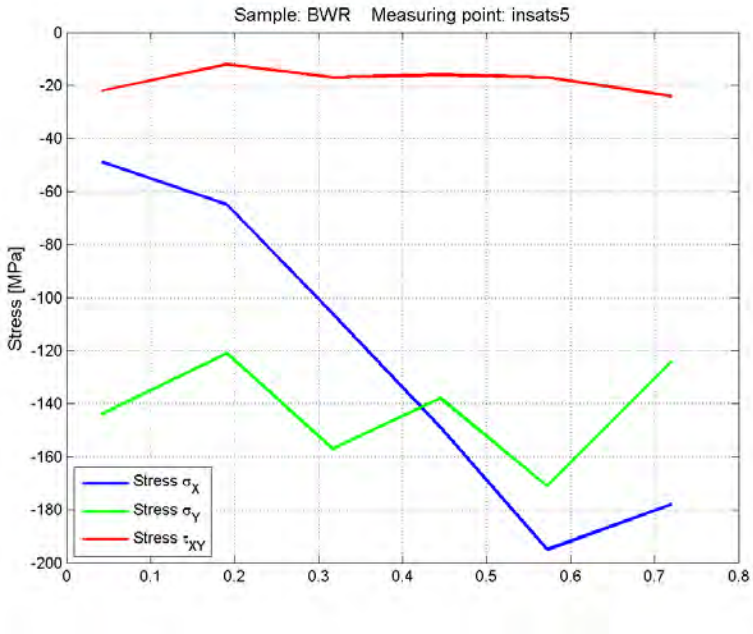

Depth mm	Hoop MPa	Axial MPa	Shear MPa	σ_e MPa
0.04	-49	-144	-22	126
0.19	-65	-121	-12	104
0.32	-106	-157	-17	138
0.45	-149	-138	-16	143
0.57	-195	-171	-17	184
0.72	-178	-124	-24	157

Figure A4: 9 Stresses calculated for the measuring point *insats5* on the sample.

Appendix 4

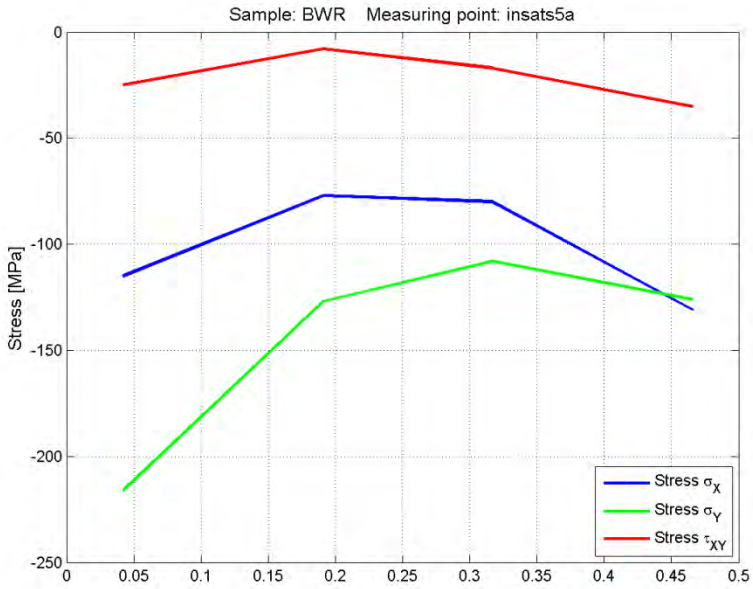

Depth mm	Hoop MPa	Axial MPa	Shear MPa	σ_e MPa
0.04	-115	-216	-25	186
0.19	-77	-127	-8	110
0.32	-80	-108	-17	96
0.47	-131	-126	-35	128

Figure A4: 10 Stresses calculated for the measuring point *insats5a* on the sample.

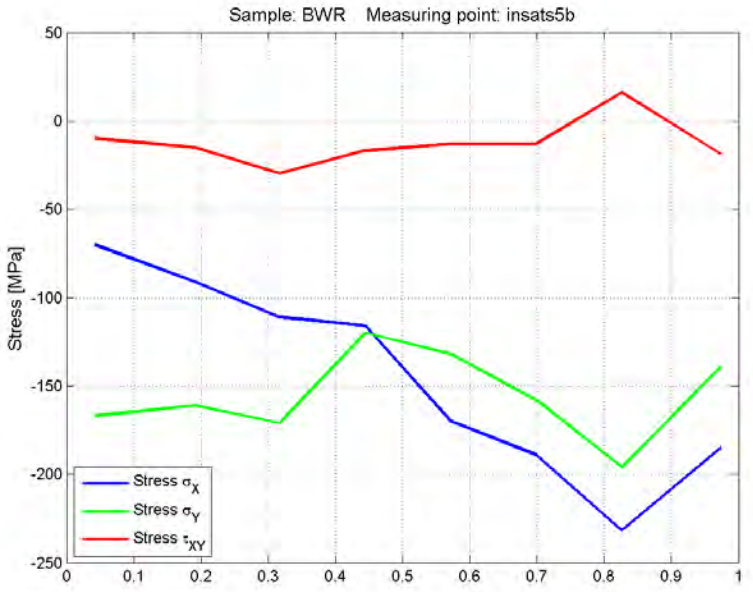

Depth mm	Hoop MPa	Axial MPa	Shear MPa	σ_e MPa
0.04	-70	-167	-10	145
0.19	-91	-161	-15	139
0.32	-111	-171	-30	149
0.45	-116	-120	-17	117
0.57	-170	-132	-13	154
0.70	-189	-158	-13	175
0.83	-232	-196	16	216
0.97	-185	-139	-19	166

Figure A4: 11 Stresses calculated for the measuring point *insats5b* on the sample. For the shaded stresses the von Mises effective stress is larger than 70% of the yield stress and therefore they are not reliable.

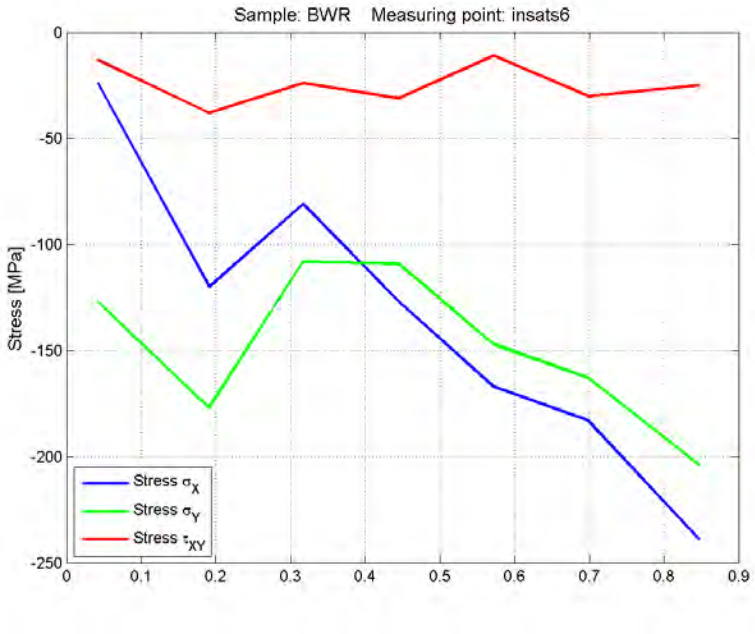

Depth mm	Hoop MPa	Axial MPa	Shear MPa	σ_e MPa
0.04	-24	-127	-13	116
0.19	-120	-177	-38	156
0.32	-81	-108	-24	96
0.45	-127	-109	-31	118
0.57	-167	-147	-11	157
0.70	-183	-163	-30	173
0.85	-239	-204	-25	223

Figure A4: 12 Stresses calculated for the measuring point *insats6* on the sample. For the shaded stresses the von Mises effective stress is larger than 70% of the yield stress and therefore they are not reliable.

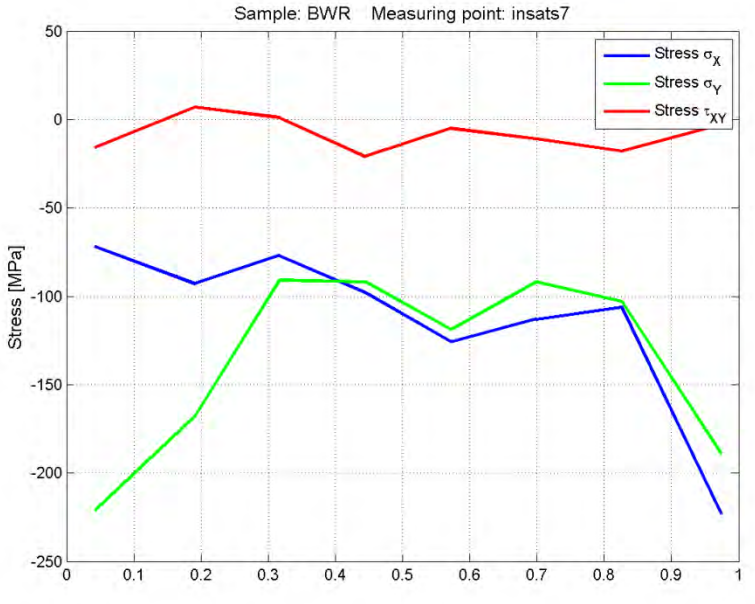

Depth mm	Hoop MPa	Axial MPa	Shear MPa	σ_e MPa
0.04	-72	-221	-16	195
0.19	-93	-168	7	145
0.32	-77	-91	1	84
0.45	-98	-92	-21	94
0.57	-126	-119	-5	122
0.70	-113	-92	-11	103
0.83	-106	-103	-18	104
0.97	-223	-189	-3	208

Figure A4: 13 Stresses calculated for the measuring point *insats7* on the sample. For the shaded stresses the von Mises effective stress is larger than 70% of the yield stress and therefore they are not reliable.

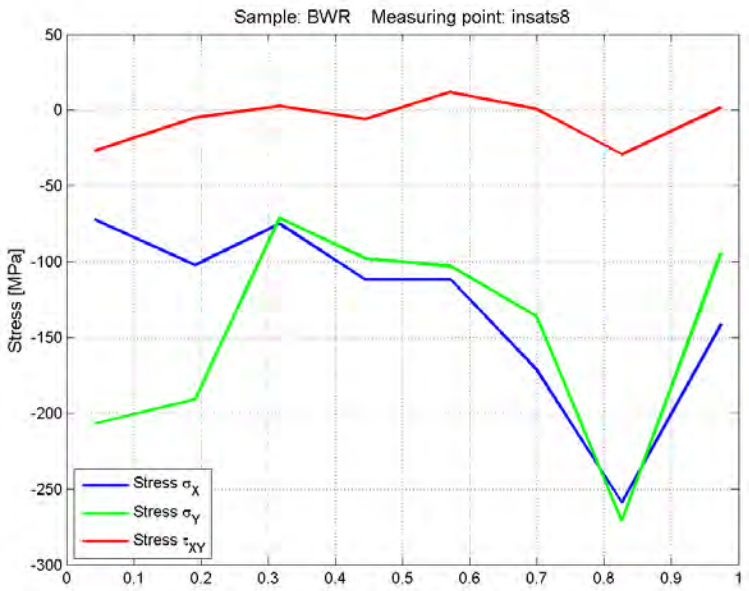

Depth mm	Hoop MPa	Axial MPa	Shear MPa	σ_e MPa
0.04	-72	-207	-27	181
0.19	-102	-191	-5	165
0.32	-75	-71	3	73
0.45	-112	-98	-6	105
0.57	-112	-103	12	107
0.70	-171	-136	1	156
0.83	-259	-271	-29	265
0.97	-141	-94	2	124

Figure A4: 14 Stresses calculated for the measuring point *insats8* on the sample. For the shaded stresses the von Mises effective stress is larger than 70% of the yield stress and therefore they are not reliable.

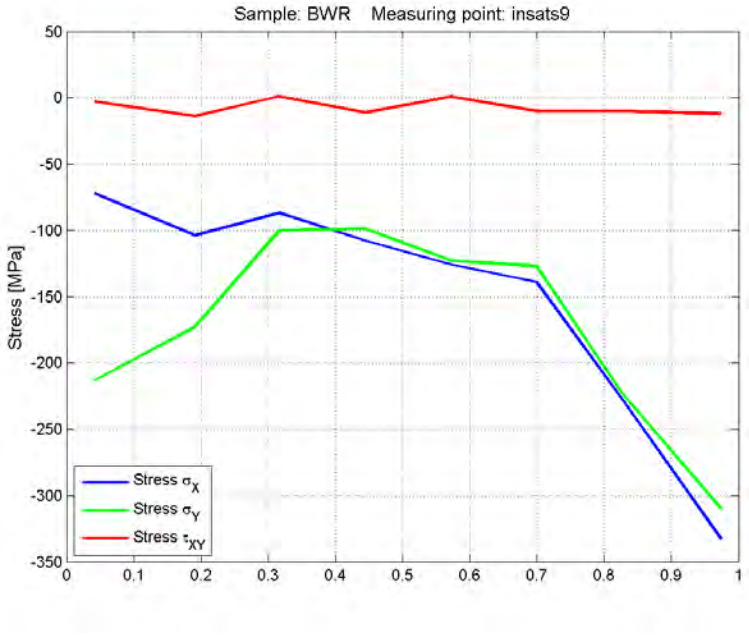

Depth mm	Hoop MPa	Axial MPa	Shear MPa	σ_e MPa
0.04	-72	-213	-3	187
0.19	-104	-173	-14	150
0.32	-87	-100	1	94
0.45	-108	-99	-11	103
0.57	-126	-123	1	124
0.70	-139	-127	-10	133
0.83	-227	-223	-10	224
0.97	-333	-310	-12	322

Figure A4: 15 Stresses calculated for the measuring point *insats9* on the sample. For the shaded stresses the von Mises effective stress is larger than 70% of the yield stress and therefore they are not reliable.